1	Gaseous ozone assisted Maillard reaction of chickpea protein isolate- arabinose:
2	Improving structural and functional properties and enhancing emulsion
3	stability
4	Xiaopeng Wei ^{a, *} , Ziyan Zhou ^a , Xiaoyuan Wang ^{a, *} , Megan Povey ^b , Guo Liu ^a , Shanshan
5	Zhang ^a , Ping Geng ^c , Lihua Zhang ^a , Zhenzhen Ge ^a
6	
7	
8	
9	
10	
11	
12	
13	^a College of Food and Bioengineering, Zhengzhou University of Light Industry, Zhengzhou, Henar
14	450000, China
15	^b University of Leeds, School of Food Science & Nutrition, Leeds, LS2 9JT, UK
16	^c College of Energy and Power Engineering, Zhengzhou University of Light Industry, Zhengzhou,
17	Henan 450000, China
18	
19	
20	
21	
22	
23	
24	* Correspond author: Xiaopeng Wei, weixiaopeng007@163.com; Xiaoyuan Wang,
25	wang459381@163.com
26	
27	
28	

Abstract

29

30

31

32

33

34

35

36

37

38

39

40

41

42

43

44

45

46

47

48

49

50

51

52

53

54

55

56

57

To break through the limitation of technological functionalities of chickpea protein isolate (CPI) in food processing conditions (e. g. high temperature and pH variations) and broaden CPI application, glycosylation modification was used to improve the structural and functional properties of CPI. Herein, ozone treatment was utilized to unfold CPI structure for promoting the Maillard reaction between CPI and arabinose (Ara). Then the influence of glycosylation modification on the structural and functional properties of CPI was investigated, and the stability of oil-in-water (O/W) emulsions loaded with β-carotene prepared with glycosylated products was evaluated. Compared to CPI, CPI pretreatment with ozone (CPI/O₃) conjugated with Ara efficiently, with a (CPI/O₃)/Ara mass ratio of 1:2, the degree of graft reached 25.3 %, suggesting the successful covalent binding of Ara to the protein. Fourier transform infrared spectroscopy (FTIR), intrinsic fluorescence spectroscopy and surface hydrophobicity analyses demonstrated that glycosylation could alter secondary and tertiary structure of CPI. Notably, the glycosylation significantly improved solubility, oil holding capacity, emulsifying properties and interfacial characteristics. Moreover, emulsions prepared with CPI/O₃-Ara conjugates, especially CPI/O₃-Ara 1:2 conjugate, showed a higher encapsulation efficiency for β-carotene, smaller droplet size, stronger ζ-potential and lower turbiscan stability index compared to emulsions made with CPI, displaying excellent stability under heating treatment and pH variation. Collectively, the results revealed that the ozone-assisted glycosylation is an efficient approach for the improvement of the functional and interfacial properties of CPI.

Keywords: Chickpea protein isolate; Arabinose; Maillard reaction; Structure characteristics; Functional properties; Interfacial features; Emulsion stability

1. Introduction

Plant-based proteins have attracted significant attention because of the lower production costs, health benefits and environmental sustainability (Grossmann & McClements, 2021). Plant proteins are mainly derived from grains and legumes. Chickpea (*Cicer arietinum* L.) is the second-largest legume crop in the word (Ke & Li, 2023), which provides an important source of protein for human beings, that is, chickpea protein isolate (CPI). In recent years, CPI is gaining recognition as a valuable protein source and sustainable alternative to animal proteins because of its nutritional

advantages, technological functionalities, economic efficiency and low allergenicity (Ma et al., 2023). CPI consists predominantly of globulin and albumin as a minor component, and displays a more compact tertiary and quaternary structure, which hinders its emulsifying capacity and stability, thereby limiting its widespread application in the food processing (Liu, Guo, Liu, Fang, et al., 2024; Wang et al., 2023). In addition, environmental factors such as high temperature, the pH value and salt concentration, can alter CPI structure and functional properties (e.g. interfacial behaviors and emulsion stability) (Liu, Guo, Fang, et al., 2024). For instance, heat treatment can cause CPI denaturation, inducing protein unfolding and disulfide bond disruption, resulting in protein aggregation (Tang et al., 2024). Therefore, property modification techniques that improve the functional properties of CPI have important theoretical instructive significance for the expansion of its application in food processing.

Currently, methods for modifying protein mainly include chemical methods, physical modification and enzymatic catalysis (Ravindran et al., 2024). Increasing studies have highlighted that pH shifting (Wang et al., 2022), cold plasma treatment (Wang et al., 2024), naringin treatment (Meng et al., 2024), high-pressure homogenization (Ma et al., 2023), ultrasonic treatment (Xu et al., 2021), atmospheric pressure plasma jet (Wang, Zhou, et al., 2023), protease hydrolysis (Kong et al, 2023; Wang, Rao, et al., 2023) can improve functional properties of CPI. Among these methods, protein glycosylation based on the Maillard reaction is recognized as a green and healthy method for improving functional properties of proteins (Basso et al., 2024). Glycosylation mainly combines the amino groups of protein molecules with the carbonyl groups of sugar molecules through hightemperature heating, thus triggering structural and functional alterations in proteins (Chaiwong et al., 2025; Han et al., 2025). As far as we know, the resulting glycosylation products display distinctive properties, with the protein absorbing on the oil-water interface rapidly, and the saccharide confers steric and electrostatic repulsion, inhibiting droplet aggregation (Li et al., 2022; Li et al., 2016). Studies have revealed that glycosylation of CPI with citrus pectin can alter structural characteristics and emulsifying properties (Liu, Guo, Fan, et al., 2024; Liu, Guo, Liu, Fan, et al., 2024; Huang et al., 2025)

In general, due to the strong steric hindrance of polysaccharides relative to monosaccharides and oligosaccharides, they are commonly used for the glycosylation with protein (Li, Wang, et al.,

2025; Li et al., 2022; Zhang et al., 2024), whereas some studies have pointed out that the structure and emulsifying capacity of glycosylated products seem to have no correlation with the chain length (Li et al., 2016; Li et al., 2013), and monosaccharides are more likely to glycosylate with proteins. Arabinose (Ara) is widely utilized in food, pharmaceutical and biological industries due to its high biological function, such as blood sugar regulation, anti-obesity and beneficial effects on gastrointestinal health (Gong et al., 2025; Wang, Zhao, et al., 2022). Chen et al. (2022) has highlighted that glycosylation of Ara with pea protein can alter the secondary structure of protein and enhance its emulsifying properties. Up till now, to obtain excellent functional properties of proteins, researchers attempt to apply physical (e. g. ultrasound and microwave) and enzymatic methods to assist Maillard glycosylation. The results have shown that ultrasound, microwave or enzyme treatments can increase the degree of glycosylation reactions via alteration of protein or polysaccharide structure, thereby improving functional properties of glycosylated products (Chaiwong et al., 2025; Liu et al., 2018; Namli et al., 2021). However, physical methods are reliant on external power, and the alteration direction is arbitrary (Kutzli et al., 2021), while enzyme methods result in the production of protein hydrolysates with unfavorable flavors (Nikbakht Nasrabadi et al., 2021). Ozone has been considered as a Generally Recognized As Safe (GRAS) chemical as early as 1997, which quickly degrades into oxygen without leaving chemical residues (Nickhil et al., 2021). Nevertheless, ozone application can enhance powder flow behavior of milk powder (Sert & Mercan, 2021) and improve functional properties of whey protein isolate (Segat et al., 2014) in the dairy processing. Importantly, studies have demonstrated that the structure of proteins undergoes alteration, for example soy protein isolate, wheat proteins and chickpea grans treated with ozone gas (Li, Chen, Wang, et al., 2025; Obadi et al., 2016; Nickhil et al., 2021). Based on the preceding observation, it is reasonable to speculate that gaseous ozone treatment may increase the degree of grafting of CPI-Ara conjugate via altering CPI structure, thus improving its functional properties.

87

88

89

90

91

92

93

94

95

96

97

98

99

100

101

102

103

104

105

106

107

108

109

110

111

112

113

114

115

In this study, ozone gas was used to pretreat CPI (CPI/O₃) to assist the glycosylation of the protein with Ara. The effect of glycosylation modification on the structure of CPI was investigated by Fourier transform infrared spectroscopy (FTIR), intrinsic fluorescence spectroscopy and surface hydrophobicity analysis; the functional and interfacial properties of CPI and CPI/O₃-Ara conjugates,

such as solubility, oil holding capacity (OHC), emulsifying properties, interfacial tension and interfacial layer thickness, were assessed; furthermore, the stability of oil-in-water (O/W) emulsions prepared with CPI and CPI/O₃-Ara conjugates were evaluated, offering new insights into the interrelationship between protein structure, interfacial adsorption, and emulsifying capacity. This study also addresses the potential for CPI/O₃-Ara conjugates as novel emulsifiers to improve the emulsion stability, thus broadening the CPI application in the food industry and providing a new technique for protein modification.

2. Materials and methods

2.1. Materials

Chickpea protein isolate (CPI, ≥ 80 %) and β-carotene were purchased from HanSuYuan Biotechnology Co., Ltd. (Shanxi, China). Arabinose (Ara, ≥ 90 %) and *o*-phenylenediamine (OPA) were purchased from Shandong Keyuan Biochemical Co., Ltd. (Shandong, China). Sunflower oil was purchased from Yihai Kerry Food Marketing Co., Ltd. (Shanghai, China). Potassium dihydrogen phosphate, sodium hydroxide and sodium chloride were purchased from Tianjin Damao Chemical Reagent Factory (Tianjing, China). Sodium dodecyl sulfate (SDS) was purchased from Tianjin Fengchuan Chemical Reagent Technology Co., Ltd. (Tianjing, China). Potassium tetraborate and n-hexane were purchased form Tianjin Kemiou Chemical Reagent Co., Ltd. (Tianjing, China). β-mercaptoethanol was purchased from Shanghai Macklin Biochemical Technology Co., Ltd. (Shanghai, China). 8-phenyl-1-naphthalene sulfonic acid (ANS) was purchased from MedChemExpress (Shanghai, China). Potassium bromide (KBr) was purchased from Shanghai Aladdin Biochemical Technology Co., Ltd. (Shanghai, China). Methanol and absolute ethanol were purchased from Tianjin Fuyu Fine Chemical Co., Ltd. (Tianjing, China). All reagents are analytical grade.

2.2. Ozone treatment

Ozone gas was produced by an ozone generator (OPV-Y100S, OPV Electrical Appliance Co., Shandong, China) and the concentration of generated ozone was 2.8 mg/L. A 4 g of CPI was added to 100 mL PBS buffer (10 M, pH 9.0), and the mixture was magnetically stirred at 25 °C for 30 min. The ozone gas was introduced into 100 mL of CPI dispersion for 1 h. Afterwards, the treated samples were placed into a refrigerator at -20 °C for 12 h and freeze-dried to obtain the ozone-treated CPI

- 145 (CPI/O_3).
- 146 2.3. Preparation of CPI/O₃-Ara conjugates
- 147 CPI/O₃-Ara conjugates were prepared using wet heating Maillard reaction (Hussain et al., 2024)
- with minor alterations. The CPI/O₃ (or CPI) and Ara were mixed at mass ratio of 3:1, 2:1, 1:1, 1:2,
- and 1:3 (w/w), and dissolved in 100 mL of deionized water. Subsequently, the mixture was stirred
- at 4 °C overnight to ensure complete dissolution. The pH of the mixture was adjusted to 7.0 and
- incubated in a water bath at 80 °C for 90 min. Soon after the heating treatment, the mixture was
- placed into an ice bath to terminate the reaction immediately. Then, the sample solution was freeze-
- dried for further analysis.
- 2.4. Degree of graft (DG) of conjugates determination
- The DG of glycosylated products was measured using the *o*-phenylenediamine (OPA) method
- 156 (Fei et al., 2025). The OPA solution was formulated by mixing 160 mg/mL of OPA reagent, 0.4 mL
- 157 of β-mercaptoethanol, 5 mL of SOS solution (1 %, w/v) and 50 mL of sodium tetraborate solution
- 158 (50 mM, pH 9.5) to the total volume of 100 mL. For DG measurement, 4 mL of OPA solution was
- added into 0.2 mL of the sample dispersion (2 mg/mL), and incubated at 35 °C for 3 min. The
- absorbance of the mixture was recorded at 340 nm using a fluorescence spectrophotometer (F-700,
- Hitachi, Japan). The DG was computed as the following equation:
- 162 $DG(\%) = [(C_0 C_t)/C_t] \times 100$
- Where C_0 and C_t are the content of free amino group of protein and glycosylated product,
- respectively.
- 165 2.5. Particle size and ζ -potential analyses
- The sample was dissolved into deionized water to a 100-fold dilution. The particle size and ζ-
- potential were measured using a laser particle size analyzer (Nano ZS 90, Malvern, UK). The
- particle size was determined at a refractive index of 1.5. All the tests were performed at 25 °C.
- 2.6. Fourier transform infrared spectroscopy (FTIR) and secondary structure analysis
- In brief, 3.0 mg of freeze-dried samples were mixed with KBr at a mass ratio of 1:100 and
- 171 grounded into fine powders. The powders were pressed and determined using a FTIR spectrometer
- 172 (Vertex 70, Bruker, Germany). The scanning range from 4000 to 400 cm⁻¹, and the results were
- analyzed with OMNIC software. Secondary structure content of samples was calculated using

- PeakFit 4.12 software (Systat Software, Inc., USA) described by Feng et al. (2025).
- 175 *2.7. Tertiary structure assay*
- 176 *2.7.1. Intrinsic fluorescence*
- The fluorescence spectrum of 0.2 mg/mL of samples was determined with a fluorescence
- 178 spectrophotometer (F-4700, Hitachi, Japan). The parameters were set as follows: excitation
- wavelength at 295 nm, scanning wavelength of 300-450 nm, and slit width of 5 nm.
- 180 2.7.2. Surface hydrophobicity (H_0)
- The H₀ was assayed according to the method of Sharifian et al. (2019). The freeze-dried
- samples were dissolved in PBS buffer (10 mM, pH 9.0) to the final concentration of 5, 25, 50, 100
- and 200 µg/mL, respectively. Then, 5 mL of sample dispersion at each concentration was added to
- 184 0.02 mL of ANS (8 mM) for 30 min. The fluorescence intensity was measured using a fluorescence
- spectrophotometer (F-4700, Hitachi, Japan) with an excitation wavelength of 385 nm and an
- emission wavelength of 480 nm. The H₀ was computed from the initial slope of RFI versus sample
- 187 concentration.
- 188 2.8. Surface morphology observation
- The surface morphology of the sample was observed using Scanning Electron Microscopy
- 190 (SEM). The freeze-dried samples (e.g. protein and emulsion) were fixed on the metal sample stage
- with the fracture surface facing up. Gold was sprayed over the surface of sample under vacuum
- environment. All sample images were recorded at room temperature with a voltage of 5 KV.
- 193 2.9. Determination of functional properties
- 194 2.9.1. Solubility and oil holding capacity (OHC)
- The sample powder was added into distilled water and stirred at room temperature for 1 h.
- After centrifugation at 5000 rpm for 20 min, the content of protein in the supernatant was determined
- using the Bradford method with bovine serum albumin (Solarbio, Beijing, China). The solubility
- was computed according to the equation:
- 199 Solubility (%) = $(m_1/m_2) \times 100$
- Where m_1 represents the content of protein in supernatant; m_2 indicates the content of protein
- in dispersion.
- The OHC was measured by the method described by Wang et al. (2024) with some

- 203 modifications. Briefly, 50 mg sample powder was mixed with 10 mL of soybean oil, and incubated
- for 30 min at 25 °C. Subsequently, the mixture was centrifuged for 20 min at 5000 rpm and discarded
- the supernatant. OHC was calculated according to the following equation:
- 206 $OHC(g/g) = (m_1-m_2)/m_2$
- Where m_1 denotes the weight after oil absorption and centrifugation; m_2 is the weight of the
- dry sample.
- 209 2.9.2. Emulsifying activity index (EAI) and emulsion stability index (ESI)
- Emulsifying properties were evaluated by determining EAI and ESI according to the methods
- of Pirestani et al. (2017). A 250 mg of sample powder was added to 20 ml of PBS buffer (10 mM),
- and then 10 ml of soybean oil was added and homogenized for 2 min. A 50 µl of emulsion was
- dispersed in SDS solution. After homogenizing, the absorbance at 500 nm was reordered, using the
- SDS solution as a blank. After waiting for 10 minutes, the absorbance value was determined again.
- The EAI and ESI were calculated as following equations:
- 216 $EAI(m^2/g) = (2 \times 2.303 \times A_0 \times DF)/(\rho \times \Phi \times (1-\theta) \times 10000$
- 217 $ESI(min) = (A_0 \times 10)/(A_0 A_{10})$
- Where DF represents the dilution factor, equaling 101; ρ denotes the concentration of protein
- 219 (g/ml); Φ is the optical path length, setting at 0.01 meters; θ indicates the percentage of the oil phase,
- which is 0.25; A_0 is the absorbance value of the sample at 0 min, while A_{10} is the absorbance value
- 221 at 10 min.
- 222 2.10. Measurement of interfacial properties
- 223 2.10.1. Interfacial tension
- The interfacial tension of the O/W interface was measured using the pendant drop method. The
- sample solution (0.1 %, w/v) was loaded into a micropipette with a 1.8 mm diameter needle, forming
- 226 a 10 μ L droplet in a 4 × 4 cm glass square filled with soybean oil. The changes in the O/W interfacial
- tension were monitored by a video optical contact angle analyzer (OCA15EC, Dataphysics,
- 228 Germany).
- 229 2.10.2. Interfacial layer thickness
- The thickness of the interfacial layer formed by CPI and CPI/O₃-Ara conjugates was analyzed
- according the method of Liu et al. (2018), with slight modifications. The polystyrene microspheres

(1 %, w/w) were diluted to 0.1 % (w/w). Then, 0.1 mL of the microsphere suspension was mixed with 0.9 mL of CPI or CPI/O₃-Ara conjugates and allowed to stand for 4 h. Subsequently, the particle sizes of the latex beads before and after sample adsorption were measured using a laser particle size analyzer (Malvern Instruments Ltd., UK). The interfacial thickness on the latex bead surface for each sample was calculated based on the difference in diameter between the latex beads with and without an adsorption of sample layer.

2.11. Preparation of O/W emulsions loaded with β-carotene

 β -carotene was dissolved in sunflower seed oil to obtain the oil phase. Subsequently the concentration of β -carotene in oil phase was determined (Liu et al., 2016). A 10 mg of CPI or CPI/O₃-Ara conjugates was added to 100 mL of deionized water and sonicated for 5 min in an icewater bath to prepare 10 mg/mL protein dispersion (aqueous phase). Afterwards, 5 mL oil phase was added in 100 mL aqueous phase and sonicated for 4 min. The resulting crude emulsions were stirred for 1 h at 35 °C to obtain O/W emulsions loaded with β -carotene.

2.12. Encapsulation efficiency (EE) measurement

The EE of β -carotene within the emulsion was assayed based on the method of Huang et al., (2022), with slight modification. A 0.2 mL of emulsion was added to 4 mL of extracting solution containing n-hexane and ethanol (1:1, v/v) and thoroughly mixed by a vortex device. After centrifugation, the absorbance value of the supernatant was reordered at 450 nm using fluorescence spectrophotometer (F-700, Hitachi, Japan) to determine β -carotene content according the method of Liu et al. (2016). The EE was copulated using the following equation:

 $EE (\%) = (C_0 - C_1)/C_0 \times 100$

Where C_1 and C_0 represent the content of free and total β-carotene, respectively.

254 2.13. Emulsion stability evaluation

255 2.13.1. Turbiscan stability

The physical stability of emulsions was determined using a Turbiscan Lab Expert (Foamulaction, France) following the method of Liu et al. (2019). The Turbiscan stability index (TSI) was computed using Turbiscan software. TSI is used to reflect the physical stability of emulsions, and an increase of TSI represents declined emulsion stability.

260 2.13.2. Thermal stability

- Emulsions were added into a centrifuge tube and incubated in a water bath at 20 °C, 40 °C,
- 262 60 °C, 80 °C, and 100 °C for 2 h, respectively. Then the particle size and ζ-potential were analyzed
- using the methods described in section 2.5.
- **264** *2.13.3. pH Stability*
- Emulsions were placed into centrifuge tubes, and the pH of emulsions was adjusted to 3, 5, 7,
- 266 9, and 11, respectively. After incubating at room temperature for 2 h, the particle size and ζ-potential
- were analyzed using the methods described in section 2.5.
- 268 2.14. Statistical analysis
- All experiments were performed in triplicate and all the data was analyzed by SPP software
- 270 (IBM SPSS Statistics 24, USA). The significance of samples was analyzed by ANOVA with
- Duncan's multiple range test. The significance level was set to P < 0.05.
- 272 3. Results and Discussion

275

- 3.1. Structure of CPI/O₃-Ara conjugates
- 3.1.1 DG of CPI/O₃-Ara conjugates
- was used to pretreat CPI. The results showed that ozone treatment could significantly reduce αHelix content companied by dramatically increase in random coil content (Fig. S1). This alteration
 of protein structure might contribute to Ara attachment onto the surface of protein. As expected,
 regardless of the mass ratio of the reactants, DG in CPI/O₃ groups was significantly higher than that

To unfold the structure of CPI for promoting the Maillard reaction between CPI and Ara, ozone

- in CPI group (Fig. 1A). This phenomenon could be attributed to the unfolding of CPI structure
- 281 caused by ozone treatment, exposing more ε -amino groups to conjugation with the carbonyl group
- of Ara. More importantly, regardless of ozone treatment, the DG of DPI/O₃-Ara conjugates was
- regulated by the mass ratio of the reactants. The DG of CPI/O₃-Ara conjugates increased gradually
- to the peak (25.3 %) at the mass ratio of 1:2 and decreased at the mass ratio of 1:3 (17.8 %). Prior
- study has shown a similar trend, the DG of CPI-citrus pectin conjugates increased firstly and then
- declined with an increase in the citrus pectin content in the reaction system (Liu, Guo, Fan, et al.,
- 287 2024). In the initial stage of the reaction, the ε-amino groups were continuously exposed due to
- heating and rapidly combined with the carbonyl group of Ara, resulting in the increased DG.
- However, increasing covalently binding of Ara to the surface of CPI/O₃ molecules hindered the

contact between the amino group and the carbonyl group. In this regard, the structure of CPI opened further as the Maillard reaction proceeded leading to a slight increase in the content of free amino acid, thus slightly reducing the DG.

3.1.2. FTIR spectroscopy and protein secondary structure

The FTIR spectra of CPI and CPI/O₃-Ara conjugates is shown in Fig. 1B. In comparation with CPI, the absorption peaks of CPI/O₃-Ara conjugates at amide I band (1600-1700 cm⁻¹) and amide II band (1480-1575 cm⁻¹) slightly shifted, indicating that the vibration of the amide groups was altered by the attachment of Ara onto CPI/O₃ (Sheng et al., 2020). Studies have pointed out that the new bonds of Schiff bases (C=N), Amadori compounds (C=O) and pyrazines (C-N), which generated by the Maillard reaction, had absorption peaks in the range of 800-1800 cm⁻¹ (Chen et al., 2019; Zhao et al., 2023). Obviously, several new absorption peaks were observed from 800 to 1800 cm⁻¹, indicating the formation of Maillard reaction products. Moreover, compared to CPI, the absorption peaks of CPI/O₃-Ara conjugates at 1013 and 3340 (or 3344) cm⁻¹ dramatically enhanced, which might be attributed to the C-O and O-H stretching vibrations resulting from Ara grafting onto the protein (Liu, Guo, Fan, et al., 2024; Spotti et al., 2019). Introduction of hydrogen groups of Ara resulted in a shift in absorption peak at 3395 cm⁻¹ (O-H), showing that the attachment of Aar onto CPI/O₃ increased the number of hydrogen groups in the Maillard reaction products. The production of new bonds, enhancement and shift in the absorption peaks suggests that CPI/O₃-Ara conjugates formed by the Maillard reaction, was consistent with the DG results.

The secondary structure of the protein can be analyzed using PeakFit software, including α -helix, β -sheet, β -turn and random coil. Typically, the α -helix is a dense ordered structure closely related to the stability of protein structure, while β -sheet and β -turn are considered as relatively extended ordered structure, and random coil is a disordered structure (Zhao et al., 2021). Fig. 1C shows the secondary structure compositions of CPI and CPI/O₃-Ara conjugates, with α -helix (30.1 %) and β -sheet (33.0 %) predominating in CPI. Compared with CPI, CPI/O₃-Ara conjugates displayed a significant reduction in the content of α -helix and slightly decrease in β -sheet and an dramatical increase in the random coil content, in accordance with the results of FTIR where the absorption peaks at amide I (yellow band at 1700-1600 cm⁻¹), including α -helix, β -sheet, β -turn, and random coil, altered evidently (Savadkoohi et al., 2016). The content of α -helix and β -sheet also

declined with the increase in DG of the CPI/O₃-Ara conjugates. The reason for this is that glycation of CPI/O₃ with Ara reduced the ϵ -amino groups in the α -helix and β -sheet regions and the involvement of lysine in glycation reaction reduced α -helix and β -sheet content (Li et al., 2014). The glycation reaction with Ara unfolded the protein secondary structure and transformed from ordered structure (α -helix and β -sheet) to flexible and looser structure (random coil), which improved the functional properties of proteins, such as emulsifying properties and surface hydrophobicity (Chen et al., 2019; Martineza et al., 2007). This finding was consistent with the results of Liu, Guo, Fan, et al. 2024, who reported a decrease in α -helix content and increase in random coil content of CPI covalently bonded with citrus pectin.

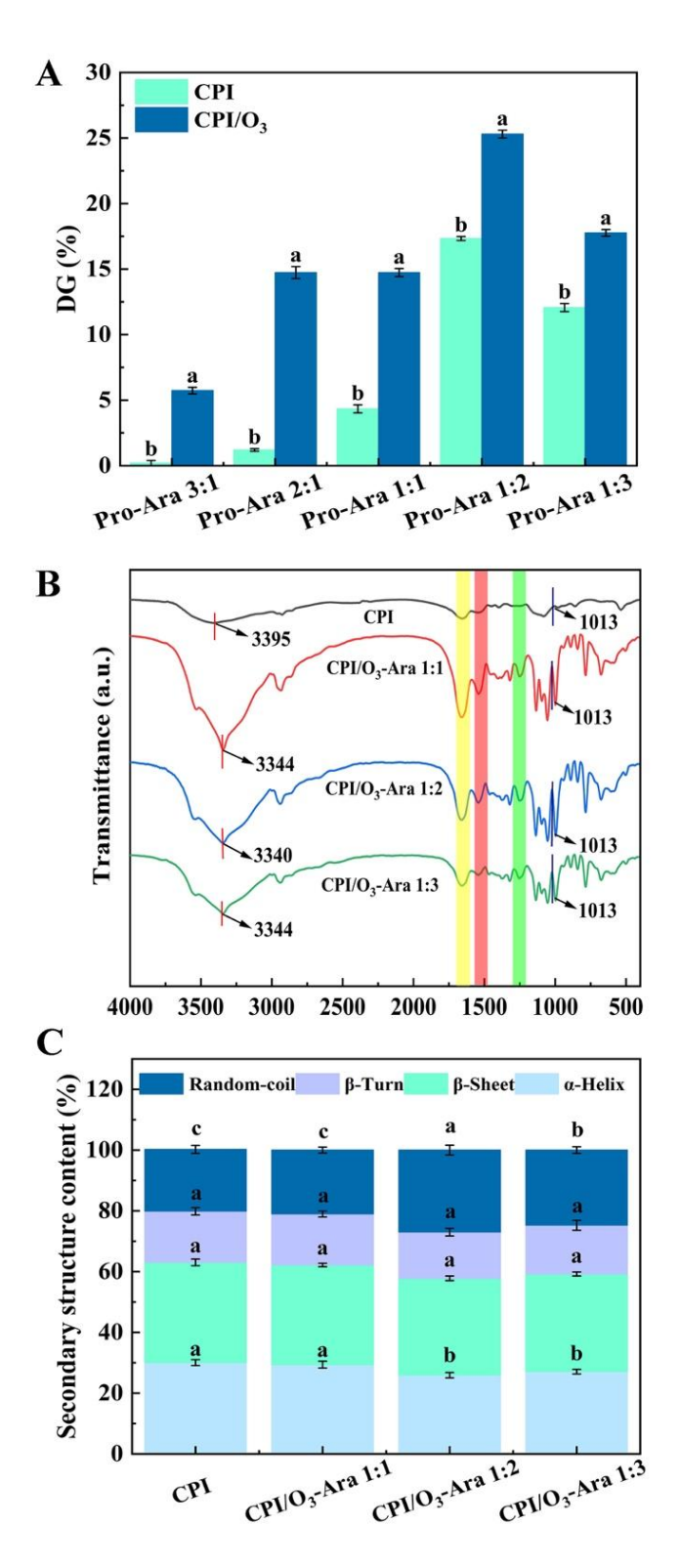


Fig. 1. A Degree of graft, **B** FTIR spectroscopy, **C** Second structure of CPI and CPI/O₃-Ara conjugates. The yellow band, red band, and green band represent amide I band (1600-1700 cm⁻¹), amide II band (1480-1575 cm⁻¹), and amide III band (1300-1200 cm⁻¹), respectively. Pro-Ara, the mass ratio of protein (CPI or CPI/O₃) and Ara. Different lowercase letters demote significant differences (P < 0.05).

3.1.3. Intrinsic fluorescence spectroscopy analysis

334

335

336

337

338

339

340

341

342

343

344

345

346

347

348

349

350

351

352

353

354

355

356

357

358

359

360

361

362

Intrinsic fluorescence spectroscopy is one of the most useful method for evaluating the microenvironment changes around the tyrosine and tryptophan residues, reflecting the tertiary structure of protein (Wang et al., 2017). It can be seen from Fig. 2A that the maximum emission wavelength of CPI was 330 nm which showed the highest fluorescence intensity. Nevertheless, the fluorescence intensity of CPI/O₃-Ara conjugates reduced sharply after glycosylation. This decrease of fluorescence intensity could be attributed to the shielding effect by introduction of hydrophilic Ara onto the protein surface (Chen et al., 2022). Another reason was because tyrosine might be involved in the glycosylation reaction with Ara, resulting in the reduction of tyrosine content and a rapid decline in fluorescence intensity (Zhang et al., 2023). Besides the decreased fluorescence intensity of CPI/O₃-Ara conjugates, a slight red shift was observed in the maximum fluorescence emission (from 330 to 331), which proved that tyrosine and tryptophan residues moved towards a more hydrophilic microenvironment. This might be due to the tertiary structure of CPI unfolding under ozone and heating treatments, causing tyrosine and tryptophan residues to expose towards a more polar microenvironment; or addition of Ara made the microenvironment around CPI/O₃ more hydrophilic. The reduction of fluorescence intensity and red shift in fluorescence peaks of CPI/O₃-Ara conjugates suggested that the glycosylation modification caused the change in CPI tertiary construe. This result was congruent with the findings of Liu, Guo, Fan, et al. (2024), who reported that glycosylation of CPI with citrus pectin caused a decrease in the fluorescence intensity and a rede shift in absorption peaks of CPI-citrus pectin conjugates.

3.1.4. Surface hydrophobicity (H_0) analysis

H₀ is strongly related to the functional properties of protein, such as emulsification, solubility and interfacial tension (Jiang et al., 2015; Li et al., 2016). H₀ values of CPI, CPI/O₃ and CPI/O₃-Ara conjugates are presented in Fig. 2B. H₀ value of CPI/O₃ (72987.3) was highest than these of other groups, which was due to that ozone treatment unfolded the structure of CPI to make the exposure of hydrophobic groups buried inside of the protein (Mahdavian Mehr & Koocheki, 2021). More importantly, glycosylation modification significantly reduced H₀ of CPI, and the value decreased from 46733.3 (CPI) to 14874.7 (CPI/O₃-Ara 1:1), 11638.0 (CPI/O₃-Ara 1:2) and 11699.0 (CPI/O₃-Ara 1:3), respectively. Obviously, H₀ value decreased as the increase in DG, consistent with the

previous study (Liu, Guo, Liu, Fan, et al., 2024). A possible explanation is that the glycosylation reaction consumed free lysine leading to the reduction of ANS binding sites (ε-amino lysine), and attachment with Ara given more hydrophilic hydroxyl groups onto the surface of CPI/O₃ molecular, causing a decrease in H₀. In addition, although the DG of CPI/O₃-Ara 1:2 conjugate was significantly higher than that of CPI/O₃-Ara 1:3 conjugate, a significant difference in H₀ between them was not observed. This was because Ara might noncovalently interact with CPI/O₃, thus hindering the binding of ANS fluorescence probe with hydrophobic residues.

3.1.5. ζ-potential and particle size

As shown in Fig. 2 C, the isoelectric point of CPI was approximately pH 4 (the ζ-potential reduced to 0 at pH 4), which is consistent with most plant proteins. After the Maillard reaction, the isoelectric points of CPI/O₃-Ara conjugates were slightly different. The potential value in all groups increased gradually from pH 5 to pH 9, followed by a slight decrease at pH 11. Overall, CPI/O₃-Ara conjugates had higher potential values between pH 5 to pH 9, especially CPI/O₃-Ara 1:2 conjugate, as compared to CPI. At pH 9, the potential value of CPI/O₃-Ara 1:2 conjugate increased to -13.7 mV, which was 1.1-fold higher than that of CPI. A strong ζ-potential can provide high electrostatic repulsion for protein molecules, hindering their aggregation and reducing particle size.

The particle sizes of CPI and CPI/O₃-Ara conjugates were shown in Fig. 2D. The particle size of the CPI group was 279.8 nm. Obviously, the Maillard reaction significantly increased the particle size of CPI, represented by CPI/O₃-Ara 1:1 of 497.6 nm, CPI/O₃-Ara 1:3 of 331.2 nm, CPI/O₃-Ara 1:2 of 370.9 nm. This increase in particle size might be due to the protein structure expansion induced by ozone and heating treatments. Furthermore, attachment of Ara based on the Maillard reaction could increase particle size, but the higher amount of Ara attached to CPI/O₃ might provide strong electrostatic and steric repulsion, avoiding protein aggregation into a larger size, which can explain why CPI/O₃-Ara 1:2 conjugate had a smaller size compared to CPI/O₃-Ara 1:3 and CPI/O₃-Ara 1:1 conjugates.

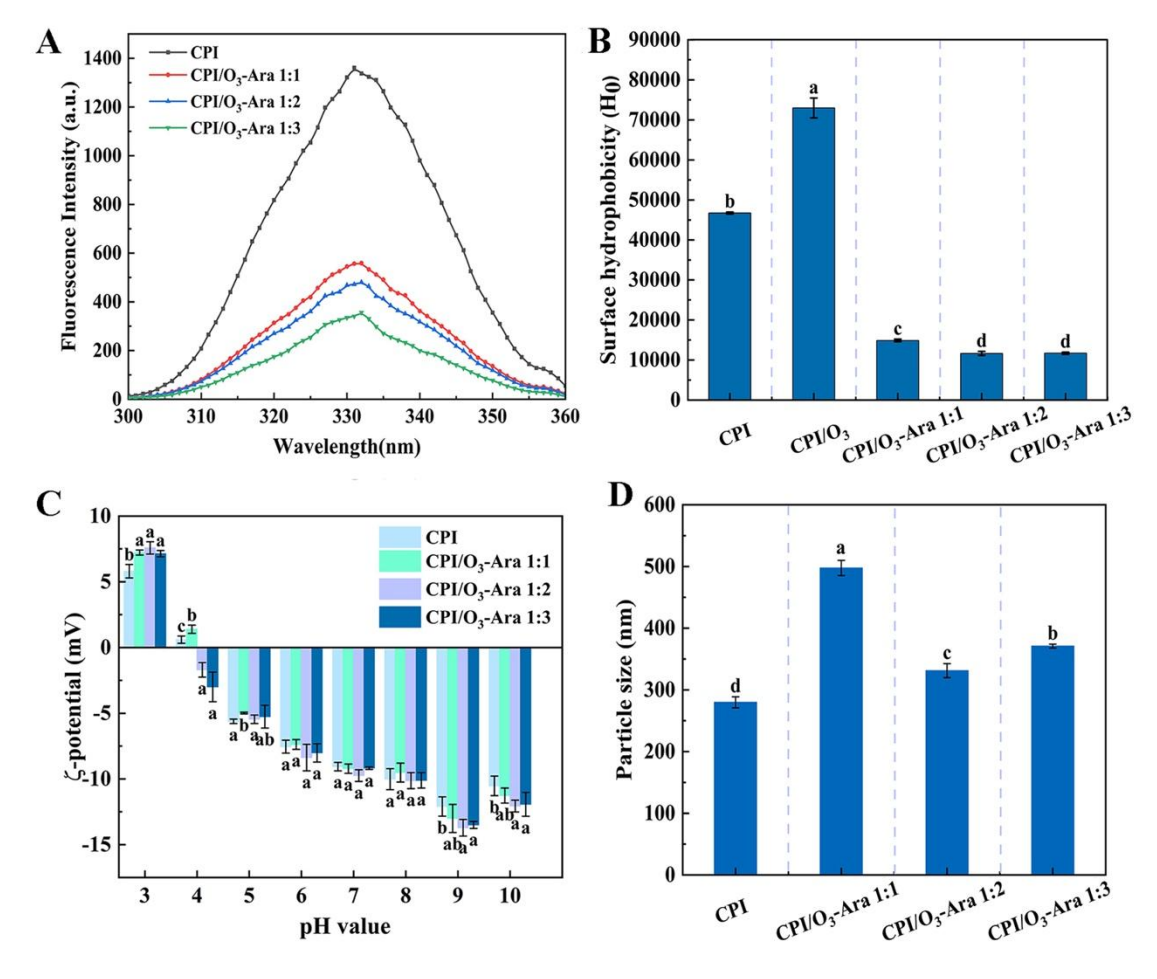


Fig. 2. A Intrinsic fluorescence spectroscopy, **B** Surface hydrophobicity (H₀), **C** ζ-potential, **D** particle size of CPI and CPI/O₃-Ara conjugates. Different lowercase letters demote significant differences (P < 0.05).

3.2 Functional characteristics of CPI/O₃-Ara conjugates

3.2.1. Solubility and oil holding capacity (OHC)

Solubility is a critical parameter that reflects the hydrophilic and hydrophobic balance of protein and also impacts on the surface functional properties, such as interfacial tension and emulsification (Li et al., 2022). As illustrated in Fig. 3A, glycosylation modification dramatically improved the solubility of CPI, and with an increase in DG, the solubility of CPI/O₃-Ara conjugates raised, reaching a peak of 5.5 mg/mL at CPI/O₃-Ara 1:2. This was possible due to attachment of hydrophilic Ara onto the protein surface, which reduced H₀ of the conjugates, thus increasing their solubility. Furthermore, the steric effect of Ara and the increased ζ-potential elevated the steric and electrostatic repulsion, preventing the aggregation and flocculation of CPI/O₃-Ara conjugates.

Similar findings were also reported for conjugates of soy protein isolate with bitter almond gum (Ghaedi & Hosseini, 2021), and binding of pea protein isolate with Ara (Chen et al., 2022).

OHC of CPI and CPI/O₃-Ara conjugates is presented in Fig. 3B. Obviously, OHC of CPI/O₃-Ara conjugates significantly exceeded that of CPI, with highest value reordered in CPI/O₃-Ara 1:2 conjugate at 3.9 g/g. A possible reason for this phenomenon might be attributed to the alteration of CPI structure via glycosylation of Ara to the protein, exposing more hydrophobic groups buried inside of the protein, which promoted the interaction between protein and oil, forming protein-oil compound (Wang et al., 2023).

3.2.2. Emulsifying properties

403

404

405

406

407

408

409

410

411

412

413

414

415

416

417

418

419

420

421

422

423

424

425

426

427

428

429

430

431

Emulsifying properties reflect the ability of proteins to form and stabilize emulsions, which can be evaluated by EAI and ESI. Recent studies have highlighted the glycosylation modification by the Maillard reaction effectively improving the emulsifying properties of conjugates (Karabulut et al., 2024). As expected, binding of Ara to CPI/O₃ enhanced EAI and ESI of the protein (Figs. 3C and 3D). Notably, EAI pronouncedly increased from 196.2 (CPI) to 207.9 (CPI/O₃-Ara 1:1), 229.4 (CPI/O₃-Ara 1:3) and 267.9 (CPI/O₃-Ara 1:2), while ESI dramatically increased from 14.0 (CPI) to 18.9 (CPI/O₃-Ara 1:1), 25.3 (CPI/O₃-Ara 1:3) and 38.5 (CPI/O₃-Ara 1:2). Moreover, EAI and ESI in CPI/O₃-Ara conjugates increased significantly with the increased DG, and CPI/O₃-Ara 1:2 conjugate showed the highest EAI and ESI, which were 1.4 and 2.8 times higher than those of CPI. In general, the emulsifying properties of proteins are tightly associated with their structural and physicochemical properties, such as secondary structure, solubility, hydrophilic-hydrophobic balance and ζ-potential (Hussain et al., 2024; Liu, Guo, Liu, Fan, et a., 2024). A study has pointed out that the looser surface structure associated with random coil structure is beneficial for Maillard conjugates which absorb quickly and firmly on the oil-water surface, improving the emulsifying properties (Li et al., 2022). In this regard, the increased EAI of CPI/O₃-Ara conjugates might be due to the increase in the content of random coil inducted by glycosylation of Ara. More importantly, introduction of hydrophilic Ara reduced H₀ and increased solubility, resulting in an equilibrium of the hydrophilic and hydrophobic ratio on the conjugates surface, which made conjugates rapidly absorb at the oil-water interface to form amphiphilic films, thereby increasing emulsion activity. Binding of plentiful hydrophilic Ara could thicken the film around the oil droplets, which had the

benefit for improving emulsion stability. Additionally, the steric effect of Ara and stronger electrostatic repulsive forces of conjugates also contribute to preventing the aggregation and flocculation of protein molecules (Chen et al., 2022; Zhang et al., 2025), thus improving emulsion stability.

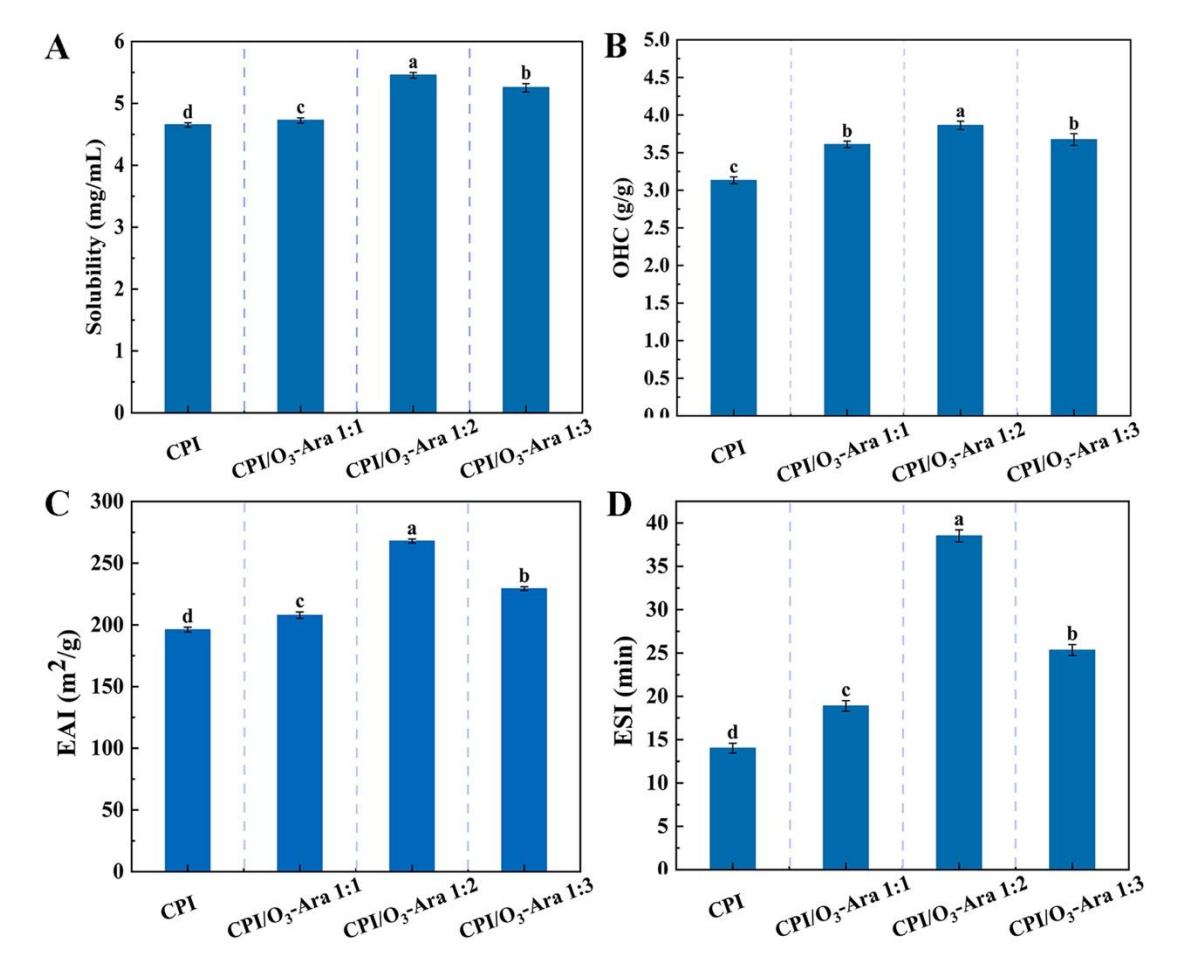


Fig. 3. A Solubility, **B** Oil holding capacity (OHC), **C** Emulsifying activity index (EAI), **D** Emulsifying stability index (ESI) of CPI and CPI/O₃-Ara conjugates. Different lowercase letters demote significant differences (P < 0.05).

3.3. Interfacial Features

Absorbed layer thickness of CPI and CPI/O₃-Ara conjugates was determined using uniform polystyrene latex as absorption surface. As shown in Fig. 4A, the interfacial layer thickness formed by CPI was 17.2 nm, while the layer thickness of CPI/O₃-Ara 1:1, CPI/O₃-Ara 1:3 and CPI/O₃-Ara 1:2 significantly increased to 21.9, 29.0 and 34.0 nm, respectively. The results were consistent with the findings of Liu et al. (2018), who reported that corn fiber gum-bovine serum albumin conjugates

formed a larger layer thickness compared to bovine serum albumin. In this study, the increase in layer thickness formed by CPI/O₃-Ara conjugates due to the covalent cross-linking of Ara with protein molecule improved the hydrophilic and hydrophytic balance and steric barrier, thus formatting a more compact absorption layer.

Interfacial tension can be used to indicate the absorption behavior of protein at the oil-water interface. As presented in Fig. 4B, the interfacial tension in all groups declined gradually with increasing time, suggesting that surface absorption was a time-dependent process. In the later stage, the interfacial tension displayed a slowly decreasing trend, indicating that the interfacial absorption became saturated gradually and reached equilibrium. Notably, grafting Ara onto CP/O₃ via the Maillard reaction dramatically decreased interfacial tension as compared to CPI. Previous studies have pointed out that grafting of hydrophilic sugar can reduced interfacial tension by improving amphiphilic balance and increasing steric stabilization and electrostatic repulsion (Fei et al., 2025; Feng et al., 2025). Evidently, in the present study, grafting Ara onto CP/O₃ was able to enhance hydrophilicity, increase ζ-potential and form compact interfacial layer, which might cooperatively decrease interface tension.

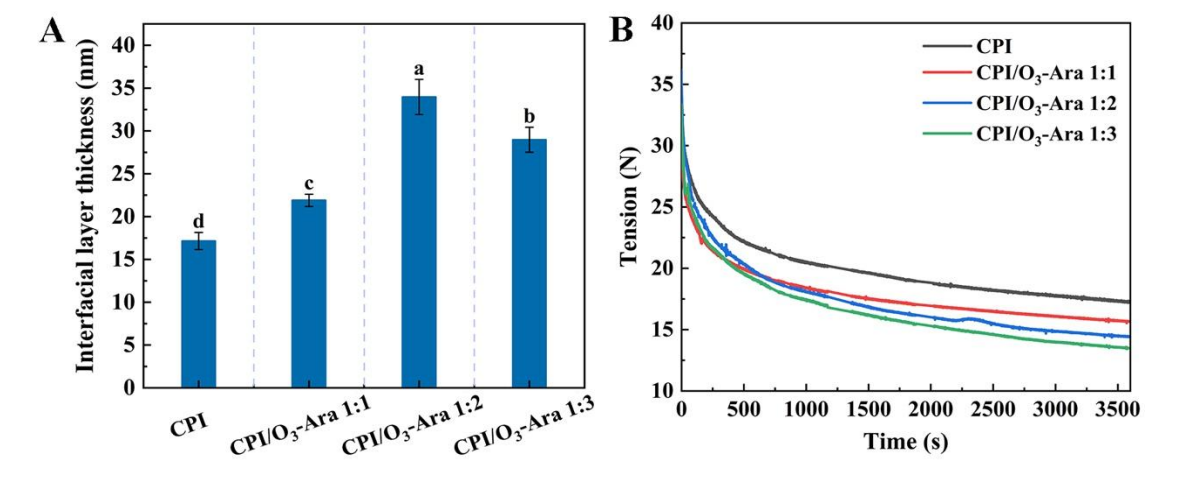


Fig. 4. A Interfacial layer thickness, **B** Interfacial tension of CPI and CPI/O₃-Ara conjugates. Different lowercase letters demote significant differences (P < 0.05).

3.4. Surface morphology observation

SEM is a common imaging technique used to observe the morphological structure of protein molecules. As shown in Fig. 5A, CPI presented a smooth spherical structure, which was consistent

with the morphology of legume protein reported by Yang et al. (2023). Obviously, ozone treatment and the Maillard reaction significantly altered the morphology; that is, CPI/O₃-Ara conjugates displayed more sheet surface structure which was open and porous (Figs. 5B-C). This was because Ara attached to the surface of CPI/O₃ let the conformation change, and ozone and heat treatments also made protein structure became unfold, which was in consistent with the results of FTIR analysis. Furthermore, the SEM images obtained for CPI/O₃-Ara conjugates appeared to be thin resembling a sheet, especially CPI/O₃-Ara 1:2 conjugate, which was because the Maillard reaction allowed Ara to open the protein structure and diminished protein aggregation (Dursun & Yalcin, 2021; Hussain et al., 2024).

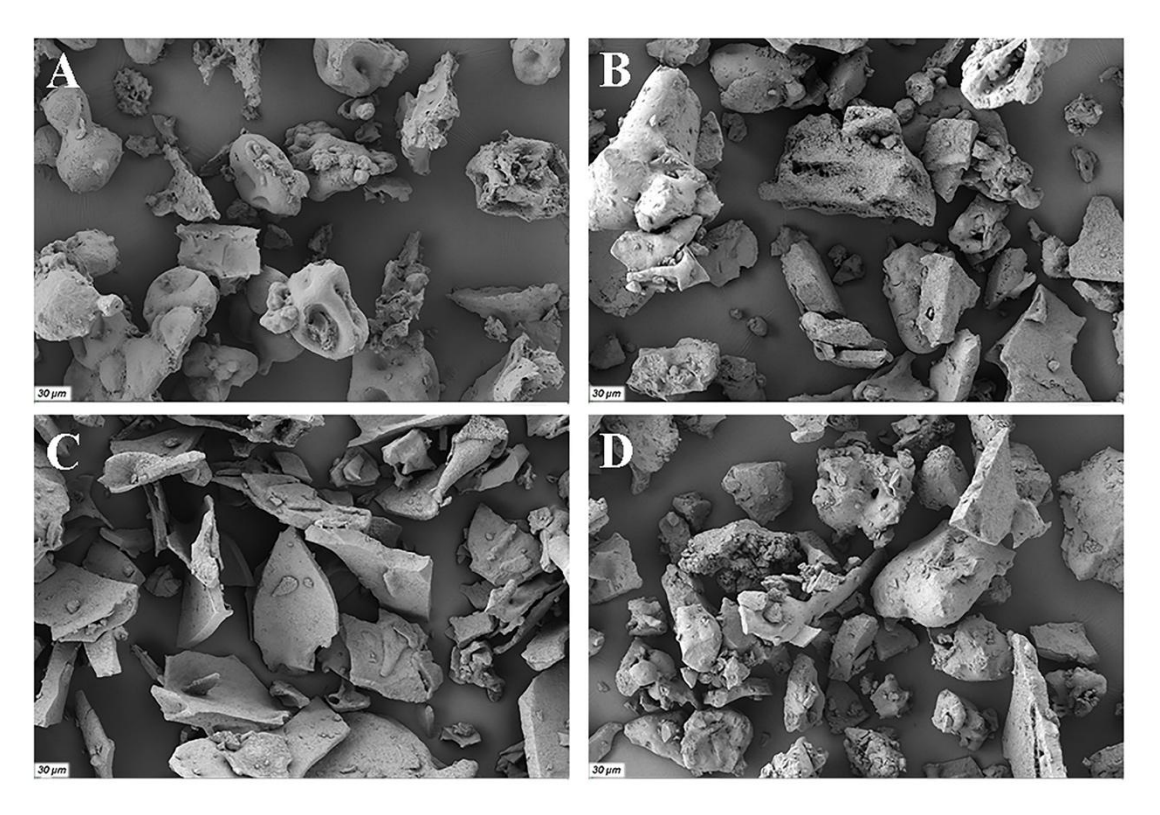


Fig. 5. Scanning electron microscopy (SEM) of CPI (**A**) and CPI/O₃-Ara conjugates. **B**, CPI/O₃-Ara 1:1 conjugate; **C**, CPI/O₃-Ara 1:2 conjugate; **D**, CPI/O₃-Ara 1:3 conjugate.

3.5 Characterization of emulsions

3.5.1. Microstructure of emulsions

The microstructure of emulsions prepared with CPI and CPI/O₃-Ara conjugates observed using SEM is shown in Fig. 6. The CPI emulsion exhibited an open and non-homogeneous structure with

evident larger and irregular pores. By contrast, CPI/O₃-Ara conjugate emulsions had denser and homogeneous structure with a relatively smoother surface. The results indicated that the structural unfolding of CPI/O₃-Ara conjugates improved the microstructure of emulsions, with more homogeneous and compact microstructure which had better oil holding and stabilizing capacity in emulsion.

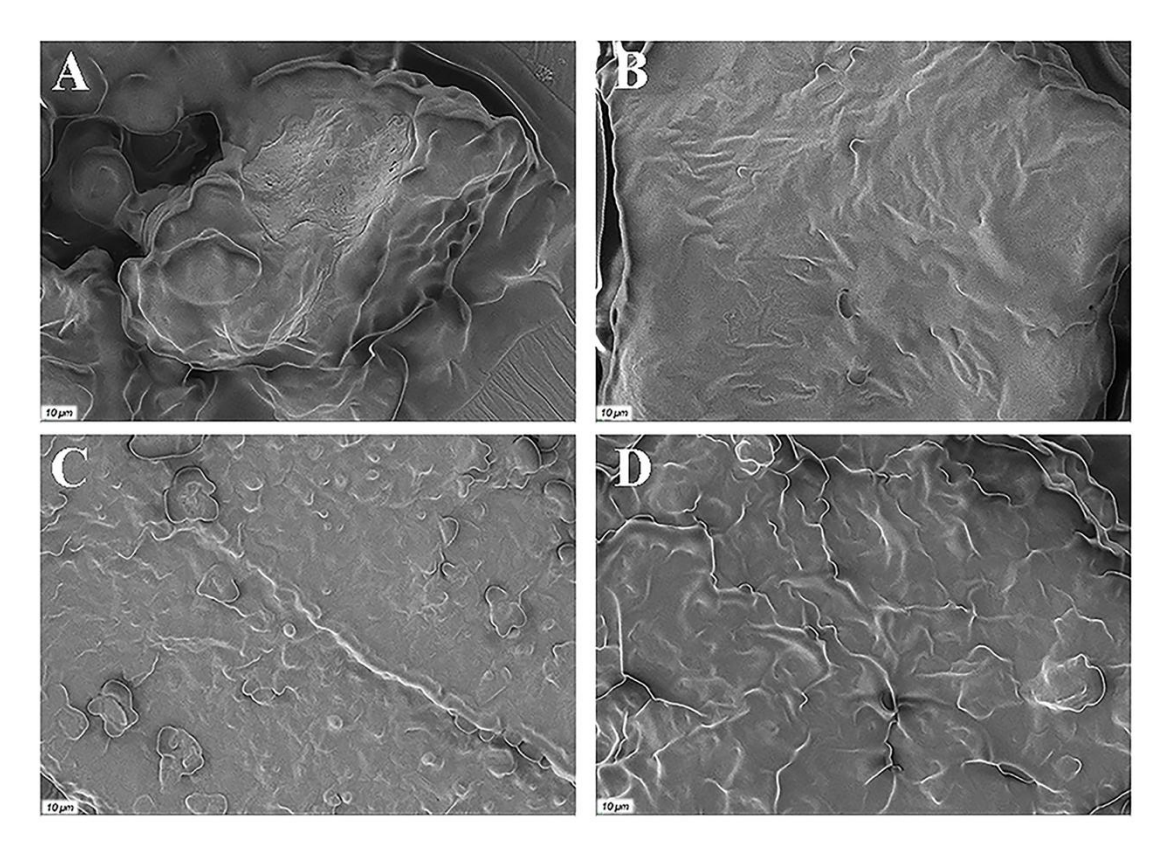


Fig. 6. Scanning electron Microscopy (SEM) of emulsions prepared with CPI and CPI/O₃-Ara conjugates. **A** emulsion stabilized by CPI, **B** emulsion stabilized by CPI/O₃-Ara 1:1 conjugate, **C** emulsion stabilized by CPI/O₃-Ara 1:2 conjugate, **D** emulsion stabilized by CPI/O₃-Ara 1:3 conjugate.

3.5.2. Encapsulation efficacy (EE), ζ-potential and particle size

The effect of glycosylation on encapsulation efficacy (EE) of β -carotene is presented in Fig. 7A. Emulsions prepared with CPI and CPI/O₃-Ara conjugates displayed high EE from 82.7 % to 90.1 %, respectively. However, glycosylation modification could significantly increase EE of β -carotene. This phenomenon was attributed to higher emulsifying capacity and OHC, and lower interface tension of CPI/O₃-Ara conjugates, enabling more β -carotene loading in oil droplets.

Moreover, the Maillard reaction unfolded the protein conformation, contributing to embedding more oil droplets, leading to the increased EE of β -carotene.

The changes in ζ -potential of emulsions prepared with CPI and CPI/O₃-Ara conjugates is shown in Fig. 7B. Emulsions made with CPI and CPI/O₃-Ara conjugates had a negative charge at the interface, which might be due to the anionic nature of the Ara and CPI at a pH above its isoelectric point. The ζ -potential value of emulsions prepared with conjugates were dramatically higher than that stabilized by CPI, following the order CPI/O₃-Ara 1:2 > CPI/O₃-Ara 1:3 > CPI/O₃-Ara 1:1 > CPI. The results were consistent with the finding of Zha et al. (2019), who reported that emulsion prepared with pea protein isolate-gum Arabic conjugate has a higher ζ -potential value compared to that of emulsion made with native protein.

As plotted in Fig. 7C, the droplet size of emulsions prepared with CPI/O₃-Ara 1:2 (343.6 μm), CPI/O₃-Ara 1:3 (362.3 μm) and CPI/O₃-Ara 1:1 (401.9 μm) was significantly smaller than that prepared with CPI (460.8 μm). As CPI/O₃-Ara conjugates had higher emulsifying properties and lower interfacial tension (Figs. 3 and 4), the emulsions made with conjugates manifested the better phase stabilization, especially CPI/O₃-Ara 1:2 conjugate. Moreover, the stronger charge and the steric effect of Ara in conjugates-stabilized emulsions hindered the droplet aggregation and its consequent increase in size.

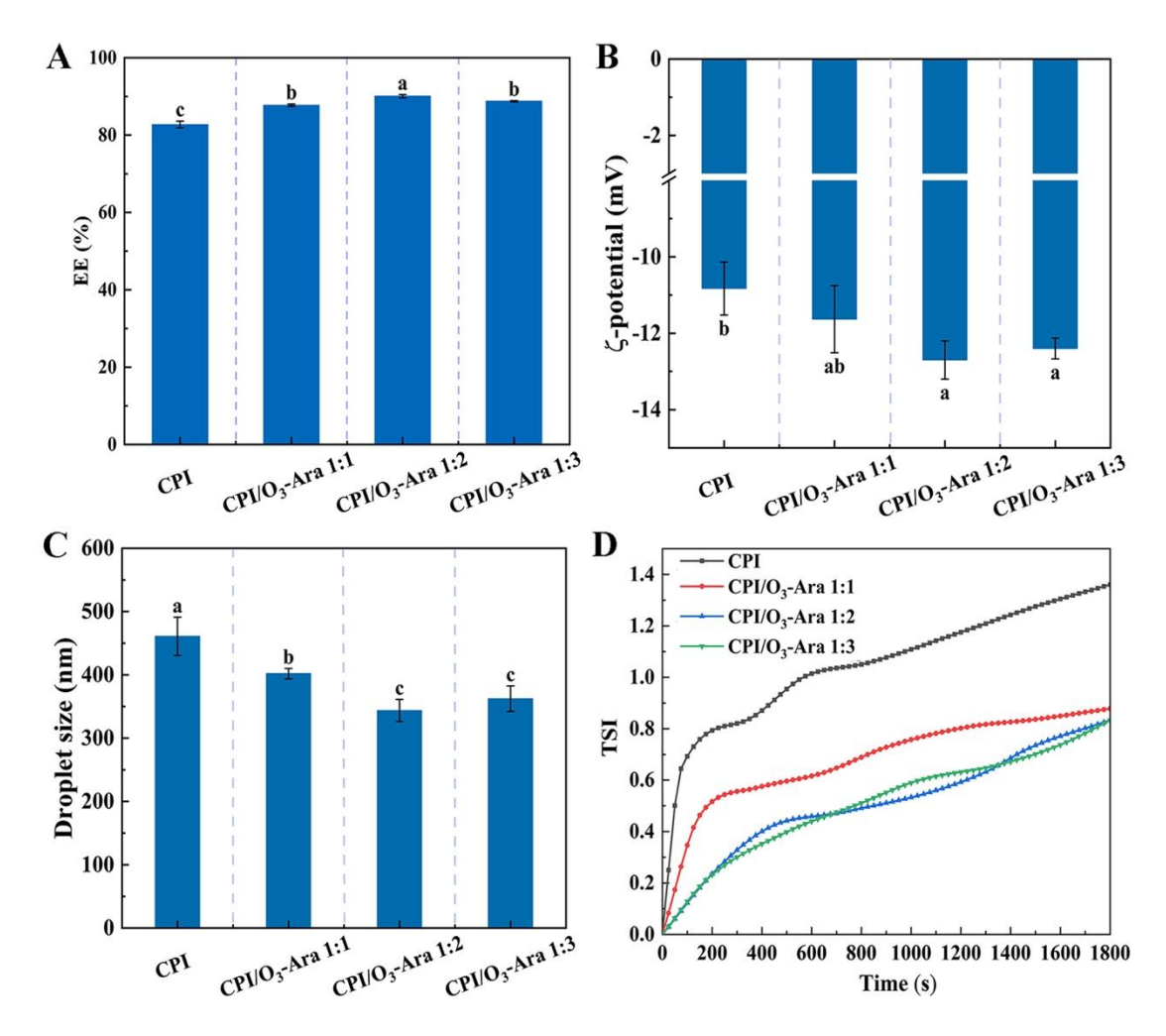


Fig. 7. A Encapsulation efficacy (EE), **B** ζ-potential, **C** particle size, **D** Turbiscan stability index (TSI) of emulsions prepared with CPI and CPI/O₃-Ara conjugates. Different lowercase letters demote significant differences (P < 0.05).

3.5.3. Emulsion stability

TSI embodies all the instability conditions such as the thickness of the clear and sediment layers, and particle sedimentation, therefore it can be utilized to evaluate physical stability of emulsion (Xu et al., 2021). As illustrated in Fig. 7D, the TSI value of emissions formed by CPI and CPI/O₃-Ara conjugates increased along with the incubation time, suggesting a decline in physical stability. This phenomenon might be due to the increase in particle size caused by the droplet aggregation and flocculation. Studies have highlighted that emulsions will display destabilization phenomenon (e.g. sediment), when the TSI value exceeds 3.0 (Jin et al., 2020). The TSI values of all emulsions were lower than 3.0 within the test time, indicating excellent physical stability.

However, compared to CPI emulsions, emulsions formed by CPI/O₃-Ara conjugates showed the lower TSI value, especially emulsions formed by CPI/O₃-Ara 1:2 and CPI/O₃-Ara 1:3. The excellent physical stability of all emulsions might be due to the strong electrostatic and steric repulsion. According to the results in Fig. 7B, all the emulsions displayed higher droplet charge, especially emulsions stabilized by CPI/O₃-Ara 1:2 and CPI/O₃-Ara 1:3. Apart from electrostatic repulsion, attachment of Ara might introduce the steric repulsion which also contributed to hindering droplet aggregation. In addition, glycosylation modification changed the structure of CPI/O₃-Ara conjugates, thereby improving their (especially CPI/O₃-Ara 1:2 and CPI/O₃-Ara 1:3 conjugates) functional and interfacial properties, such as ESI and interfacial layer thickness, which were beneficial for the physical stability.

Thermal treatments are key steps in food processing, such as boiling and sterilization. Therefore, investigating the thermal stability of CPI and CPI/O₃-Ara conjugates emulsions is essential to assess proteins application in food processing. As shown in Fig. 8 A, the droplet size of all protein emulsions increased with temperature increase. The droplet size of CPI emulsion increased to 587.9 μ m, while CPI/O₃-Ara conjugates emulsions displayed lower droplet size, in particular, CPI/O₃-Ara 1:2 emulsion increased only by 404.1 μ m. Heat treatment causes protein denaturation, leading to droplet aggregation or flocculation (Setiowati et al., 2020). Moreover, heat treatment altered the structure of proteins, decreasing in the negativity of ζ -potential (Fig. 8B). CPI/O₃-conjugates had higher emulsifying capacity, lower interfacial tension and thicker interfacial layer, which made them absorb at the oil-water interface rapidly and form a compact and thick interface layer, thus enhancing the thermal stability.

Changes in pH can alter the conformation and ζ -potential of protein molecules, which affect their ability to absorb at the oil-water interface and emulsion stability (Liu, Guo, Fan, et al., 2024). The stability of emulsions prepared with CPI and CPI/O₃-Ara conjugates was assessed across a range from pH 3.0 to pH 11.0 (Fig. 8C). Under acidic conditions, the droplet size of CPI protein emulsions increased significantly, from 928.3 nm to 7683.3 nm, reaching a peak near the isoelectric point, consistent with the ζ -potential of protein and conjugates (Fig. 2C). In contrast, CPI/O₃-Ara conjugate emulsions had a lower droplet size. Under alkaline conditions, the droplet size of all emulsions significantly decreased and remained at a stable level (< 460 nm), while emulsions

stabilized by CPI/O₃-Ara conjugates had lower droplet size (< 400 nm) when compared to that of CPI emulsion. At pH 3.0, ζ -potential of all emulsions showed positive values, in line with the fact that proteins carry positive charges below their isoelectric point. Over the pH range 5.0-11.0, the ζ -potential of all emulsions became negative, and the absolute value increased to a peak at pH 9.0, followed by a decreasing trend at pH 11.0. The enhanced pH stability of CPI/O₃-Ara emulsions can be attributed to the repulsive forces generated by electrostatic interactions and steric effect of Ara, preventing the droplet aggregation.

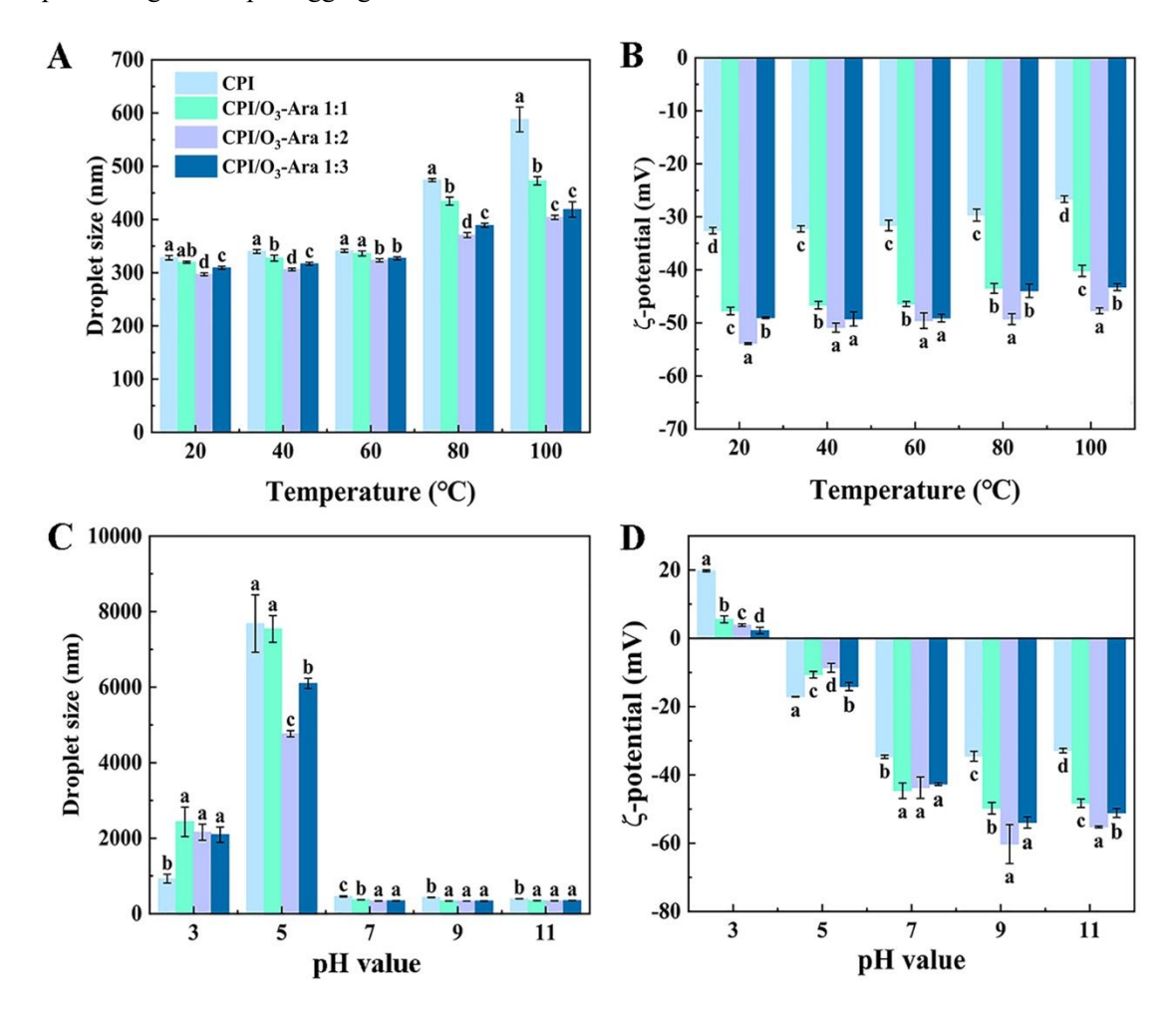


Fig. 8. Effect of thermal treatment on particle size (**A**) and ζ-potential (**B**); effect of pH value on particle size (**C**) and ζ-potential (**D**) of emulsions stabilized by CPI and CPI/O₃-Ara conjugates. Different lowercase letters demote significant differences (P < 0.05).

4. Conclusion

To broaden the application of CPI in food industry, this study attempts to improve functional and interfacial properties via glycosylation modification of CPI based on the Maillard reaction.

Ozone pretreatment increased the DG of CPI/O₃-Ara conjugates via altering the secondary structure of the protein. The DG and FTIR analyses verified the covalent binding of CPI/O₃ to Ara. The Maillard reaction induced the structure alteration of CPI, including the secondary and tertiary structure. The changes in the structure induced by the Maillard reaction improved the functional and interfacial properties of CPI/O₃-Ara conjugates, represented by the decrease in surface hydrophobicity and interfacial tension, and the increase in solubility, oil holding capacity, emulsifying properties and thickness of interfacial layer. It was worth noting that among the CPI/O₃-Ara conjugates, their functional and interfacial properties were positive correlated with the DG; that is CPI/O₃-Ara 1:2 conjugate have better properties with a higher DG when compared to CPI/O₃-Ara 1:3 and CPI/O₃-Ara 1:1 conjugates. Furthermore, the stability of emulsions made with CPI/O₃-Ara conjugates, especially CPI/O₃-Ara 1:2 conjugate, were higher than that of CPI emulsion under varying conditions (i.e., TSI, heating treatment and different pH value), probably due to an increase in interfacial layer thickness and emulsifying properties, and enhancement of steric effect of Ara and electrostatic repulsion, resulting in smaller droplet size and stronger ζ-potential of emulsions. Collectively, this study offers an innovative technique for chemical modification of protein, and CPI/O₃-Ara conjugate is promising as a novel protein emulsifier. Further study would use CPI/O₃-Ara conjugates as emulsifiers for food processing; for instance, using CPI/O₃-Ara conjugates to prepare O/W emulations loaded fat-soluble nutrients (e. g. β-carotene, vitamin D and vitamin E) add into fruit juice, thus improving its nutritive value.

Declaration of competing interest

The authors declare that they have no conflict of interest.

Acknowledgments

- This study was supported by Key Research and Development Project of Henan Province
- **601** (241111111800) and the Natural Science Foundation of Henan Province (252300421433).

References

578

579

580

581

582

583

584

585

586

587

588

589

590

591

592

593

594

595

596

597

599

602

- Basso, F., Manzocco, L., Saraiva, J. A., & Nicoli, M. C. (2024). A kinetic study on the effect of
- hyperbaric storage on the development of Maillard reaction in glucose-glycine model systems.
- Innovative Food Science and Emerging Technologies, 92, Article 103603.
- https://doi.org/10.1016/j.ifset.2024.103603

- Chaiwon, N., Gavahian, M., Tridtitanakiat, P. C., Therdtatha, P., Moukamnerd, C., Leksawasdi, N.,
- & Phimolsiripol, Y. (2025). Ultrasound-accelerated Maillard reaction to improve functional
- and antioxidant properties of hemp protein-carboxymethyl chitosan conjugates as a future food
- 610 ingredient. Innovative Food Science and Emerging Technologies, 104, Article 104118.
- https://doi.org/10.1016/j.ifset.2025.104118
- 612 Chen, W. J., Ma, X. B., Wang, W. J., Lv, R. L., Guo, M. M., Ding, T., Ye, X. Q., Miao, S., & Liu, D.
- H. (2019). Preparation of modified whey protein isolate with gum acacia by ultrasound
- 614 Maillard reaction. Food Hydrocolloids, 95, 298-307.
- https://doi.org/10.1016/j.foodhyd.2018.10.030
- 616 Chen, X., Dai, Y. J., Huang, Z., Zhao, L. W., Du, J., Li, W., & Yu, D. Y. (2022). Effect of ultrasound
- on the glycosylation reaction of pea protein isolate-arabinose: Structure and emulsifying
- properties. Ultrasonics Sonochemistry, 89, Article 106157.
- https://doi.org/10.1016/j.ultsonch.2022.106157
- Dursun Capar, T., & Yalcin, H. (2021). Protein/polysaccharide conjugation via Maillard reactions
- in an aqueous media: Impact of protein type, reaction time and temperature. LWT-Food Science
- *and Technology*, 152, Article 112252. https://doi.org/10.1016/j.lwt.2021.112252
- 623 Fei, X. Y., Xue, H., Chen, H. T., Dai, T. T., Gong, D., & Zhang, G. W. (2025). Glycosylation of whey
- protein-gallic acid conjugates with pectin: Improved emulsifying property and interfacial
- behavior. Food Research International, 218, Article 116875.
- https://doi.org/10.1016/j.foodres.2025.116875
- 627 Feng, J. Z., Li, Z. Y., Luan, C., Huang, J. C., Zheng, M. J., Wang, Z. H., Chen, Y. Q., & Yang, J.
- 628 (2025). Structural characterization and emulsification properties of quinoa protein-dextran
- 629 conjugates fabricated through ultrasound-assisted Maillard reaction. Food Chemistry, 478,
- Article 143601. https://doi.org/10.1016/j.foodchem.2025.143601
- 631 Gong T., Liao, L. Z., Tang, Y., Liu, W. W., Yao, L., Wu, Z., Li, J. M., Bai, F. L., Zhang, Q., & Tang,
- L. L. (2025). L-arabinose alleviates constipation through gastrointestinal peptide, gut
- microbiota, and Phlpp2 of gastrointestinal rhythms in rats. Journal of Functional Foods, 125,
- Article 106697. https://doi.org/10.1016/j.jff.2025.106697
- Grossmann, L., & McClements, D. J. (2021). The science of plant-based foods: approaches to create

- nutritious and sustainable plant-based cheese analogs. Trends in Food Science & Technology,
- 637 118, 207-229. https://doi.org/10.1016/j.tifs.2021.10.004.
- 638 Han, J. H., Keum, D. H., Lee, H. J., Kim, Y. J., Jung, H. S., Kim, D. H., Kwon, H. C., Shin, D. M.,
- & Han, S. G. (2025). Ultrasound-assisted Maillard reaction of *Corynebacterium glutamicum*
- protein: Impact on structure, taste, and plant-based meat applications. Ultrasonics
- 641 *Sonochemistry*, 120, Article 107424. https://doi.org/10.1016/j.ultsonch.2025.107424
- 642 Huang, Z., Zeng, Y. J., Wu, X. L., Li, M. F., Zong, M. H., & Lou, W. Y. (2022). Development of
- 643 *Millettia speciosa* champ polysaccharide conjugate stabilized oil-in-water emulsion for oral
- delivery of β-carotene: Protection effect and in vitro digestion fate. Food Chemistry, 397,
- Article 133764. https://doi.org/10.1016/j.foodchem.2022.133764
- Hussain, A., Hussain, M., Ashraf, W., Karim, A., Aqeel, S. M., Khan, A., Hussain, A., Khan, S, &
- Zhang, L. F. (2024). Preparation, characterization and functional evaluation of soy protein
- 648 isolate-peach gum conjugates prepared by wet heating Maillard reaction. Food Research
- 649 *International*, 192, Article 114681. https://doi.org/10.1016/j.foodres.2024.114681
- 650 Jiang, L. Z., Wang, Z. J., Li, Y., Meng, X. H., Sui, X. N., Qi, B. K., & Zhou, L. Y. (2015).
- Relationship between surface hydrophobicity and structure of soy protein isolate subjected to
- different ionic strength. *International Journal of Food Properties*, 18(5), 1059-1074.
- https://doi.org/10.1080/10942912.2013.865057
- 654 Jin, W. P., Wang, A. F., Peng, D. F., Shen, W. Y., Zhu, Z. Z., Cheng, S. Y., Li, B., & Huang, Q. R.
- 655 (2020). Effect of pulsed electric field on assembly structure of α-amylase and pectin
- 656 electrostatic complexes. Food Hydrocolloids, 101, Article 105547.
- https://doi.org/10.1016/j.foodhyd.2019.105547
- Karabulut, G., Goksen, G., & Khaneghah, A. M. (2024). Plant-based protein modification strategies
- towards challenges. Journal of Agriculture and Food Research, 15, Article 101017.
- https://doi.org/10.1016/j.jafr.2024.101017
- Ke, C. X., & Li, L. (2023). Influence mechanism of polysaccharides induced Maillard reaction on
- plant proteins structure and functional properties: A review. Carbohydrate Polymers, 302,
- Article 120430. https://doi.org/10.1016/j.carbpol.2022.120430
- Kong, Y., Toh, N. P., Wu, Y. Y., & Huang, D. J. (2023). Trypsin-treated chickpea protein hydrolysate

- enhances the cytoaffinity of microbeads for cultured meat application. Food Research
- 666 International, 173, Article 113299. https://doi.org/10.1016/j.foodres.2023.113299
- Kutzli, I., Weiss, J., & Gibis, M. (2021). Glycation of plant proteins via maillard reaction: reaction
- chemistry, technofunctional properties, and potential food application. Foods, 10(2), Article
- 378. https://doi.org/10.3390/foods10020376
- Li, C., Xue, H. R., Chen, Z. Y., Ding, Q., & Wang, X. G. (2014). Comparative studies on the
- physicochemical properties of peanut protein isolate-polysaccharide conjugates prepared by
- description of ultrasonic treatment or classical heating. Food Research International, 57, 1-7.
- https://doi.org/10.1016/j.foodres.2013.12.038
- 674 Li, J. Y., Chen, Y Q., Wang, D., Yin, L. J., Lv, C Y., Zang, J. C., Zhao, G. H., & Zhang, T. (2025).
- Ozone treatment increase the whiteness of soy protein isolate through the degradation of
- 676 isoflavone. Food Chemistry, 464, Article 141665.
- https://doi.org/10.1016/j.foodchem.2024.141665
- Li, S. X., Wang, C. Y., Dai, Y. Y., Dai, J. Q., & Wang, W. T. (2025). Novel technologies, effects and
- applications of modified plant proteins by Maillard reaction and strategies for regulation: A
- 680 review. Food Research International, 204, Article 115959.
- https://doi.org/10.1016/j.foodres.2025.115959
- Liu, C., Bhattarai, M., Mikkonen, K. S., & Heinonen, M. (2019). Effects of enzymatic hydrolysis
- of fava bean protein isolate by alcalase on the physical and oxidative stability of oil-in-water
- emulsions. Journal of Agricultural and Food Chemistry, 67, 6625-6632.
- https://doi.10.1021/acs.jafc.9b00914
- Liu, Y. B., Guo, X. B., Fan, X. M., Yu, X. Y., Liu, T., & Zhang, J. (2024). Improving the emulsifying
- properties and oil-water interfacial behaviors of chickpea protein isolates through Maillard
- reaction with citrus pectin. *International Journal of Biological Macromolecules*, 283, Article
- 689 137671. https://doi.org/10.1016/j.ijbiomac.2024.137671
- Liu, F. G., Ma, C. C., McClements, D. J., & Gao, Y. X. (2016). Development of polyphenol-protein-
- polysaccharide ternary complexes as emulsifiers for nutraceutical emulsions: Impact on
- formation, stability, and bioaccessibility of β-carotene emulsions. Food Hydrocolloids, 61,
- Article 578e588. https://doi.org/10.1016/j.foodhyd.2016.05.031

- 694 Liu, Y. B., Guo, X. B. Liu, T., Fan, X. M., Yu, X. Y., & Zhang, J. (2024). Study on the structural
- characteristics and emulsifying properties of chickpea protein isolate-citrus pectin conjugates
- prepared by Maillard reaction. International Journal of Biological Macromolecules, 264,
- Article 130606. https://doi.org/10.1016/j.ijbiomac.2024.130606
- 698 Liu, Y., Yadav, M. P., & Yin, L. J. (2018). Enzymatic catalyzed corn fiber gum-bovine serum
- albumin conjugates: Their interfacial adsorption behaviors in oil-in-water emulsions. Food
- 700 *Hydrocolloids*, 77, Article 986e994. https://doi.org/10.1016/j.foodhyd.2017.11.048
- 701 Li, W. W., Zhao, H. B., He, Z. Y., Zeng, M. M., Qin, F., & Chen, J. (2016). Modification of soy
- protein hydrolysates by Maillard reaction: Effects of carbohydrate chain length on structural
- and interfacial properties. Colloids and Surfaces B: Biointerfaces, 138, 70-77.
- 704 https://doi.org/10.1016/j.colsurfb.2015.11.038
- Li, Y., Zhong, F., Ji, W., Yokoyama, W., Shoemaker, C. F., Zhu, S., & Xia, W. S. (2013). Functional
- properties of Maillard reaction products of rice protein hydrolysates with mono-, oligo- and
- 707 polysaccharides. Food Hydrocolloids, 30, Article 53e60.
- 708 https://doi.org/10.1016/j.foodhyd.2012.04.013
- 709 Li, Z. Q., Xi, J., Chen, H. M., Chen, W. J., Chen, W. X., Zhong, Q. P., & Zhang, M. (2022). Effect
- of glycosylation with apple pectin, citrus pectin, mango pectin and sugar beet pectin on the
- 711 physicochemical, interfacial and emulsifying properties of coconut protein isolate. Food
- 712 Research International, 156, Article 111363. https://doi.org/10.1016/j.foodres.2022.111363
- 713 Mahdavian Mehr, H., & Koocheki, A. (2021). Physicochemical properties of Grass pea (*Lathyrus*
- sativus L.) protein nanoparticles fabricated by cold atmospheric-pressure plasma. Food
- 715 *Hydrocolloids*, 112, Article 106328. https://doi.org/10.1016/j.foodhyd.2020.106328
- Martineza, K. D., Sanchezb, C. C., Ruiz-Henestrosab, V. P., Patinob, R., Juan, M., & Pilosof, A. M.
- R. (2007). Effect of limited hydrolysis of soy protein on the interactions with polysaccharides
- 718 at the air-water interface. Food Hydrocolloids, 21(5-6), 813-822.
- 719 https://doi.org/10.1016/j.foodhyd.2006.09.008
- 720 Ma, Y. G., Zhang, J., He, J. M., Xu, Y. J., & Guo, X. B. (2023). Effects of high-pressure
- homogenization on the physicochemical, foaming, and emulsifying properties of chickpea
- 722 protein. Food Research International, 170, Article 112986.

- 723 https://doi.org/10.1016/j.foodres.2023.112986
- Meng, Y., Wei, Z. H., & Xue, C. H. (2024). Correlation among molecular structure, air/water
- interfacial behavior and foam properties of naringin-treated chickpea protein isolates. Food
- 726 *Hydrocolloids*, 147, Article 109309. https://doi.org/10.1016/j.foodhyd.2023.109309
- Namli, S., Sumnu, S. G., & Oztop, M. H. (2021). Microwave glycation of soy protein isolate with
- rare sugar (D-allulose), fructose and glucose. Food Bioscience, 40, Article 100897.
- 729 https://doi.org/10.1016/j.fbio.2021.100897
- 730 Nickhil, C., Mohapatra, D., Kar, A., Giri, S. K., Tripathi, M. K., & Sharma, Y. (2021). Gaseous
- ozone treatment of chickpea grains, part I: Effect on protein, amino acid, fatty acid, mineral
- 732 content, and microstructure. Food Chemistry, 345, Article 128850.
- 733 https://doi.org/10.1016/j.foodchem.2020.128850
- Nikbakht Nasrabadi, M., Sedaghat Doost, A., & Mezzeng, R. (2021). Modification approaches of
- plant-based proteins to improve their techno-functionality and use in food products. Food
- 736 *Hydrocolloids*, 118, Article 106789. https://doi.org/10.1016/j. foodhyd.2021.106789.
- 737 Obadi, M., Zhu, K. X., Peng, W., Ammar, A. F., & Zhou, H. M. (2016). Effect of ozone gas
- processing on physical and chemical properties of wheat proteins. Tropical Journal of
- 739 Pharmaceutical Research October, 15(10), 2147-2154
- 740 http://dx.doi.org/10.4314/tjpr.v15i10.13
- Pirestani, S., Nasirpour, A., Keramat, J., & Desobry, S. (2017). Effect of glycosylation with gum
- arabic by Maillard reaction in a liquid system on the emulsifying properties of canola protein
- 743 isolate. *Carbohydrate Polymers*, 2017, 157, 1620-1627.
- 744 https://doi.org/10.1016/j.carbpol.2016.11.044
- Ravindran, N., Singh, S. K., & Singha, P. (2024). A comprehensive review on the recent trends in
- extractions, pretreatments and modifications of plant-based proteins. Food Research
- 747 *International*, 190, Article 114575. https://doi.org/10.1016/j.foodres.2024.114575
- 748 Savadkoohi, S., Bannikova, A., Mantri, N., & Kasapis, S. (2016). Structural modification in
- condensed soy glycinin systems following application of high pressure. Food Hydrocolloids,
- 750 *53*, 115-124. https://doi.org/10.1016/j.foodhyd.2014.07.028.
- 751 Segat, A., Biasutti, M., Iacumin, L., Comi, G., Baruzzi, F., Carboni, C., & Innocente, N. (2014). Use

- of ozone in production chain of high moisture mozzarella cheese. LWT-Food Science and
- 753 *Technology*, 55, Article 513e520. https://doi.org/10.1016/j.lwt.2013.10.029
- 754 Sert, D., & Mercan, E. (2021). Assessment of powder flow, functional and micro-biological
- characteristics of ozone-treated skim milk powder. *International Dairy Journal*, 121, Article
- 756 105121. https://doi.org/10.1016/j.idairyj.2021.105121
- 757 Setiowati, A. D., Wijaya, W., & Van der Meeren, P. (2020). Whey protein-polysaccharide conjugates
- obtained via dry heat treatment to improve the heat stability of whey protein stabilized
- 759 emulsions. Trends in Food Science & Technology, 98, 150-161.
- 760 https://doi.org/10.1016/j.tifs.2020.02.011.
- 761 Sharifian, A., Soltanizadeh, N., & Abbaszadeh, R. (2019). Effects of dielectric barrier discharge
- plasma on the physicochemical and functional properties of myofibrillar proteins. *Innovative*
- Food science and Emerging Technologies, 54, 1-8. https://doi.org/10.1016/j.ifset.2019.03.006
- Sheng, L., Tang, G. Y., Wang, Q., Zou, J., Ma, M. H., & Huang, X. (2020). Molecular characteristics
- and foaming properties of ovalbumin-pullulan conjugates through the Maillard reaction. *Food*
- 766 *Hydrocolloids*, 100, Article 105384. https://doi.org/10.1016/j.foodhyd.2019.105384
- 767 Spotti, M. J., Loyeau, P. A., Marangón, A., Noir, H., Rubiolo, A. C., & Carrara, C. R. (2019).
- Influence of Maillard reaction extent on acid induced gels of whey proteins and dextrans. *Food*
- 769 *Hydrocolloids*, 91, 224-231. https://doi.org/10.1016/j. foodhyd.2019.01.020
- 770 Tang, Q., Roos, Y. H., Vahedikia, N., & Miao, S. (2024). Evaluation on pH-dependent thermal
- gelation performance of chickpea, pea protein, and casein micelles. *Food Hydrocolloids*, 149,
- 772 Article 109618. https://doi.org/10.1016/j.foodhyd.2023.109618
- 773 Wang, C., Rao, J. H., Li, X. Y., He, D. H., Zhang, T., Xu, J. T., Chen, X., Wang, L., Yuan, Y., & Zhu,
- X. W. (2023). Chickpea protein hydrolysate as a novel plant-based cryoprotectant in frozen
- surimi: insights into protein structure integrity and gelling behaviors. Food Research
- 776 *International*, 169, Article 112871. https://doi.org/10.1016/j.foodres.2023.112871
- Wang, K. Q., Sun, D. W., Pu, H. B., & Wei, Q. Y. (2017). Principles and applications of spectroscopic
- techniques for evaluating food protein conformational changes: a review. Trends in Food
- 779 *Science & Technology*, 67, 207-219. https://doi.org/10.1016/j.tifs.2017.06.015
- 780 Wang, J., Zhao, H., Liu, P., Yasri, N., Zhong, N., Kibria, M. G., & Hu, J. G. (2022). Selective

- superoxide radical generation for glucose photoreforming into arabinose. *Journal of Energy*
- 782 *Chemistry*, 74, 324-331. https://doi.org/10.1016/j.jechem.2022.07.028
- 783 Wang, J., Zhou, X. Y., Ju, S. L., Cai, R. Y., Roopesh, M. S., Pan, D. D., & Du, L. H. (2023). Influence
- of atmospheric pressure plasma jet on the structural, functional and digestive properties of
- chickpea protein isolate. Food Research International, 174, Article 113565. https://doi.org/
- 786 10.1016/j.foodres.2023.113565
- Wang, J., Zhou, X. Y., Li, J. Q., Pan, D. D., & Du, L. H. (2024). Enhancing the functionalities of
- 788 chickpea protein isolate through a combined strategy with pH-shifting and cold plasma
- 789 treatment. Innovative Food Science and Emerging Technologies, 93, Article 103607.
- 790 https://doi.org/10.1016/j.ifset.2024.103607
- Wang, Y., Wang, S., Li, R., Wang, Y., Xiang, Q., Li, K., & Bai, Y. (2022). Effects of combined
- 792 treatment with ultrasound and pH shifting on foaming properties of chickpea protein isolate,
- 793 Food Hydrocolloids, 124, Article 107351. https://doi.org/10.1016/j. foodhyd.2021.107351.
- Xu, L. P., Yan, W. Q., Zhang, M., Hong, X., Liu, Y. F., & Li, J. W. (2021). Application of ultrasound
- in stabilizing of Antarctic krill oil by modified chickpea protein isolate and ginseng saponin.
- 796 LWT-Food Science and Technology, 149, Article 111803.
- 797 https://doi.org/10.1016/j.lwt.2021.111803
- 798 Yang, J. J., Zhu, B., Lu, K. Y., Dou, J. J., Ning, Y. J., Wang, H., Li, Y., Qi, B. K., & Jiang, L. Z.
- 799 (2023). Construction and characterization of Pickering emulsions stabilized by soy protein
- hydrolysate microgel particles and quercetin-loaded performance in vitro digestion. Food
- 801 Research International, 169, Article 112844. https://doi.org/10.1016/j.foodres.2023.112844
- Zha, F. C., Dong, S. Y., Rao, J. J., & Chen, B. C. (2019). Pea protein isolate-gum Arabic Maillard
- conjugates improves physical and oxidative stability of oil-in-water emulsions. Food
- 804 *Chemistry*, 285, 130-138. https://doi.org/10.1016/j.foodchem.2019.01.151
- Zhang, M., Fan, L. P., Liu, Y. F., & Li, J. W. (2023). Effects of alkali treatment on structural and
- functional properties of chickpea protein isolate and its interaction with gallic acid: To improve
- the physicochemical stability of water-in-oil emulsions. Food Hydrocolloids, 140, Article
- 808 108601. https://doi.org/10.1016/j.foodhyd.2023.108601
- Zhang, X. Y., Wang, Y., Li, Z. Y., Li, Y., & Qi, B. K. (2024). Effects of polysaccharide type on the

910	structure, interface behavior, and foam properties of soybean protein isolate hydrolysate-
811	polysaccharide Maillard conjugates. Food Hydrocolloids, 151, Article 109801.
812	https://doi.org/10.1016/j.foodhyd.2024.109801
813	Zhao, C. B., Chu, Z. J., Mao, Y. X., Xu, Y. F., Fei, P., Zhang, H., Xu, X. Y., Wu, Y. Z., Zheng, M. Z.,
814	& Liu J. S. (2023). Structural characteristics and acid-induced emulsion gel properties of
815	heated soy protein isolate-soy oligosaccharide glycation conjugates. Food Hydrocolloids, 137,
816	Article 108408. https://doi.org/10.1016/j.foodhyd.2022.108408
817	Zhao, Q., Lin, J., Wang, C., Yousaf, L., Xue, Y., & Shen, Q. (2021). Protein structural properties and
818	proteomic analysis of rice during storage at different temperatures. Food Chemistry, 361,
819	Article 130028. https://doi.org/10.1016/j.foodchem.2021.130028
820	